Renormalization of impurity scattering in one-dimensional interacting electron systems in magnetic field

T. Hikihara,[1,2] A. Furusaki,[2] and K. A. Matveev[3,*]

[1]*Division of Physics, Graduate School of Science, Hokkaido University, Sapporo, 060-0810, Japan*
[2]*Condensed Matter Theory Laboratory, RIKEN, Wako, Saitama 351-0198, Japan*
[3]*Materials Science Division, Argonne National Laboratory, Argonne, Illinois 60439, USA*

We study the renormalization of a single impurity potential in one-dimensional interacting electron systems in the presence of magnetic field. Using the bosonization technique and Bethe ansatz solutions, we determine the renormalization group flow diagram for the amplitudes of scattering of up- and down-spin electrons by the impurity in a quantum wire at low electron density and in the Hubbard model at less than half filling. In the absence of magnetic field the repulsive interactions are known to enhance backscattering and make the impurity potential impenetrable in the low-energy limit. On the contrary, we show that in a strong magnetic field the interaction may suppress the backscattering of majority-spin electrons by the impurity potential in the vicinity of the weak-potential fixed point. This implies that in a certain temperature range the impurity becomes almost transparent for the majority-spin electrons while it is impenetrable for the minority-spin ones. The impurity potential can thus have a strong spin-filtering effect.

I. INTRODUCTION

Quantum transport in one-dimensional (1D) electron systems has been a subject of great interest for many years. In one dimension the interplay between electron-electron interaction and residual disorder is a crucial factor determining transport properties. It is well known that the repulsive interactions between electrons strongly enhance the backscattering of electrons by impurities at low temperature.[1,2] This phenomenon is a manifestation of the fact that 1D electron systems at low temperatures become Tomonaga-Luttinger (TL) liquids, with properties very different from those of conventional Fermi liquids. The renormalizations of the electron scattering by impurities have been observed experimentally by measuring temperature or bias dependence of the conductance of quantum wires[3,4] and carbon nanotubes.[5,6]

In this paper we explore the TL-liquid renormalizations of the potential of a single impurity in the presence of a strong magnetic field B. Such a field causes significant polarization of electron spins. This polarization modifies the low-energy properties of the TL liquid, resulting in qualitatively different renormalization group (RG) flows of electron backscattering by the impurity. In particular, when the energy band is less (more) than half filled, repulsive interactions may *decrease* the backscattering of majority-spin electrons (holes) in the vicinity of the weak-impurity fixed point, while increasing that of minority-spin electrons (holes). This can be thought of as enhancement of a spin-filtering effect due to interactions.

Renormalizations of the electron scattering by an impurity at zero magnetic field has been studied analytically in the limiting cases of weak and strong scatterer.[1,2] The magnitude of the impurity scattering of spin-λ electrons ($\lambda = \uparrow, \downarrow$) is characterized by a small backscattering amplitude v_λ in the former limit, and by a small amplitude t_λ of tunneling through the impurity potential in the latter one. The interac-

tions between electrons give rise to power-law renormalizations of these amplitudes at low temperatures

$$v_\lambda \propto \left(\frac{T}{D}\right)^{\alpha_\lambda}, \quad t_\lambda \propto \left(\frac{T}{D}\right)^{\beta_\lambda}, \tag{1}$$

where T is the temperature and D is the bandwidth. The exponents α_λ and β_λ at $B=0$ are determined by the electron-electron interactions. The repulsive interactions result in $\alpha_\uparrow = \alpha_\downarrow < 0$ and $\beta_\uparrow = \beta_\downarrow > 0$. Thus, as the temperature T is lowered, the scattering of electrons by an impurity is enhanced in both the weak and strong impurity limits.[1,2]

Quantitative results[1,2] for the exponents α_λ and β_λ have been obtained by using the bosonization technique. This method provides a convenient description of the low-energy properties of 1D electron systems in terms of bosonic fields $\phi_\lambda(x)$ and $\Pi_\lambda(x)$ satisfying the commutation relations

$$[\phi_\lambda(x), \Pi_{\lambda'}(x')] = i\delta_{\lambda\lambda'}\delta(x-x'). \tag{2}$$

The effective Hamiltonian at $B=0$ has the spin-charge separated form $H=H_\rho + H_\sigma$ with

$$H_\rho = \int \mathcal{H}_\rho dx, \quad \mathcal{H}_\rho = \frac{\hbar u_\rho}{2\pi}\left(\pi^2 K_\rho \Pi_\rho^2 + \frac{1}{K_\rho}(\partial_x \phi_\rho)^2\right), \tag{3}$$

$$H_\sigma = \int \mathcal{H}_\sigma dx, \quad \mathcal{H}_\sigma = \frac{\hbar u_\sigma}{2\pi}\left(\pi^2 K_\sigma \Pi_\sigma^2 + \frac{1}{K_\sigma}(\partial_x \phi_\sigma)^2\right). \tag{4}$$

Here the fields $\phi_{\rho,\sigma} = (\phi_\uparrow \pm \phi_\downarrow)/\sqrt{2}$ and $\Pi_{\rho,\sigma} = (\Pi_\uparrow \pm \Pi_\downarrow)/\sqrt{2}$ describe excitations of the charge and spin modes, u_ρ and u_σ are the velocities of the charge and spin excitations, and K_ρ and K_σ are the TL-liquid parameters. It is known that for repulsive interactions K_ρ is smaller than 1, while K_σ scales to 1 at low energies as required by the SU(2) symmetry of the problem.[7,8]

The results (1) for the renormalizations of the impurity potential are obtained by adding to the Hamiltonian the perturbations describing the impurity scattering and tunneling processes, and then studying their scaling dimensions. At $B = 0$ the exponents are related to the TL-liquid parameters as

$$\alpha_\lambda = \frac{K_\rho + K_\sigma}{2} - 1, \quad \beta_\lambda = \frac{1}{2}\left(\frac{1}{K_\rho} + \frac{1}{K_\sigma}\right) - 1. \quad (5)$$

Hence, at $K_\rho < 1$ and $K_\sigma = 1$, the exponent α_λ is negative while β_λ is positive. It is interesting, however, that if the condition $K_\sigma = 1$ imposed by the SU(2) symmetry of the problem is relaxed, the sign of the exponents α_λ and β_λ may change depending on the value of $K_\rho < 1$. For example, for a system with spin anisotropy resulting in $K_\sigma > 1$ and $2 - K_\sigma < K_\rho < K_\sigma/(2K_\sigma - 1)$, one has $\alpha_\lambda > 0$ and $\beta_\lambda > 0$.[2,1,9] In this case, the potential of a weak impurity becomes an irrelevant perturbation, and the strength of the scatterer scales to zero at low temperatures. On the other hand, a scatterer with strength exceeding a certain critical value grows at $T \to 0$, as indicated by positive exponent β_λ.

This analysis suggests that the renormalizations of impurity potential may lead to a suppression of a weak impurity when a magnetic field is applied to break the SU(2) symmetry. However, the effect of magnetic field cannot be correctly described by using the Hamiltonian (3) and (4) since the spin-charge separation in the 1D system is destroyed by the magnetic field.[10,11] Thus, in order to understand the dependence of the exponents α_λ and β_λ on magnetic field, it is necessary to generalize the low-energy Hamiltonian to the case $B \neq 0$. Such a generalization was accomplished in Ref. 12 where the effective Hamiltonian for weakly interacting electrons was obtained as a Gaussian model consisting of two independent branches of bosonic excitations. Using the effective Hamiltonian, one can investigate the scaling of both the weak backscattering due to an impurity, and weak tunneling through the impurity potential. We will see that if the magnetic field is sufficiently strong, a spin-filtering phenomenon, in which the impurity blocks the transport of minority-spin charge carriers and only weakly scatters the majority-spin ones, can be realized in a certain regime of the RG flow.

The paper is organized as follows. We discuss the bosonization approach to 1D interacting electron systems in a magnetic field in Sec. II. The general form of the effective Hamiltonian is presented in Sec. II A. In Sec. II B, we obtain the parameters in the effective Hamiltonian for the 1D Hubbard model from their Bethe ansatz integral equations. In Sec. II C, we derive the effective Hamiltonian for a model describing quantum wires at low electron density. In Sec. III we discuss the renormalization of impurity potential v_λ. The scaling dimensions of the impurity potential and tunneling operators are calculated in four limiting cases in Sec. III A. The RG flow diagrams are discussed in Sec. III B. Section IV is devoted to summary.

II. EFFECTIVE HAMILTONIAN

A. Bosonization approach

In this section we review the low-energy effective theory of 1D interacting electrons in a magnetic field, following and extending the bosonization approach introduced by Penc and Sólyom.[12] This will be the basis of our analysis in the following sections.

To construct the low-energy theory, we first take the noninteracting part of the Hamiltonian and linearize the dispersions around the Fermi points $\pm k_{F\lambda}$. The electron-field operators are expressed in terms of chiral fields as

$$\Psi_\lambda(x) = e^{ik_{F\lambda}x}\Psi_{R\lambda}(x) + e^{-ik_{F\lambda}x}\Psi_{L\lambda}(x), \quad (6)$$

where $\Psi_{R\lambda}$ ($\Psi_{L\lambda}$) is the field of right- (left-) moving electrons of spin λ. Following the standard procedure,[7,8] the chiral fields are bosonized as

$$\Psi_{P\lambda}(x) = \frac{\kappa_\lambda}{\sqrt{2\pi a}} e^{is_P\varphi_{P\lambda}(x)}, \quad (7)$$

where

$$s_P = \begin{cases} + & \text{for } P = R, \\ - & \text{for } P = L, \end{cases} \quad (8)$$

κ_λ is the Klein factor satisfying $\{\kappa_\lambda, \kappa_{\lambda'}\} = 2\delta_{\lambda\lambda'}$, and $\kappa_\lambda^\dagger = \kappa_\lambda$, and a is a short-distance cutoff. The bosonic fields obey commutation relations

$$[\varphi_{P\lambda}(x), \varphi_{P\lambda'}(y)] = i\pi s_P \delta_{\lambda\lambda'} \, \text{sgn}(x - y),$$

$$[\varphi_{R\lambda}(x), \varphi_{L\lambda'}(y)] = -i\pi\delta_{\lambda\lambda'}. \quad (9)$$

The Hamiltonian density of noninteracting electrons is given in terms of the chiral fields by

$$\mathcal{H}_0 = \frac{\hbar}{4\pi}\sum_\lambda u_\lambda[(\partial_x\varphi_{R\lambda})^2 + (\partial_x\varphi_{L\lambda})^2], \quad (10)$$

where $u_\lambda > 0$ are the velocities of the linearized dispersion of the spin-λ branch.

The interactions between electrons result in two-particle scattering processes. In the most general case, they can be classified[13] into the following four types: backward scattering (the g_1 process), forward scattering (g_2), Umklapp scattering (g_3), and scattering within one branch (g_4). Among these scattering processes, the g_1 interaction between electrons with opposite spins can be discarded since $k_{F\uparrow} \neq k_{F\downarrow}$. The g_1 interaction between electrons with equal spins is equivalent to the g_2 scattering. Furthermore, since the electron density is assumed to be incommensurate with the lattice, the Umklapp (g_3) scattering can be ignored. As a result, the most general form of the quadratic part of the interaction Hamiltonian density reads

$$\mathcal{H}_{\text{int}} = \frac{\hbar}{8\pi^2}\sum_{\lambda,P}\left(g_{2\lambda}\frac{d\varphi_{P\lambda}}{dx}\frac{d\varphi_{\bar{P}\lambda}}{dx} + g_{2\perp}\frac{d\varphi_{P\lambda}}{dx}\frac{d\varphi_{\bar{P}\bar{\lambda}}}{dx}\right.$$
$$\left. + g_{4\lambda}\frac{d\varphi_{P\lambda}}{dx}\frac{d\varphi_{P\lambda}}{dx} + g_{4\perp}\frac{d\varphi_{P\lambda}}{dx}\frac{d\varphi_{P\bar{\lambda}}}{dx}\right), \quad (11)$$

where the coupling constants $g_{i\lambda,\perp}$ are real, and

$$\bar{\lambda} = \begin{cases} \downarrow & \text{for } \lambda = \uparrow, \\ \uparrow & \text{for } \lambda = \downarrow, \end{cases} \qquad \bar{P} = \begin{cases} L & \text{for } P = R, \\ R & \text{for } P = L. \end{cases} \qquad (12)$$

Combining Eqs. (10) and (11), we find the total effective Hamiltonian density written in the matrix form

$$\tilde{\mathcal{H}} = \mathcal{H}_0 + \mathcal{H}_{\text{int}} = \frac{\hbar}{4\pi} \partial_x \boldsymbol{\varphi}^T(x) \hat{\mathcal{H}} \partial_x \boldsymbol{\varphi}(x), \qquad (13)$$

where $\boldsymbol{\varphi}^T = (\varphi_{R\uparrow}, \varphi_{L\uparrow}, \varphi_{R\downarrow}, \varphi_{L\downarrow})$,

$$\hat{\mathcal{H}} = \begin{pmatrix} u_\uparrow + \tilde{g}_{4\uparrow} & \tilde{g}_{2\uparrow} & \tilde{g}_{4\perp} & \tilde{g}_{2\perp} \\ \tilde{g}_{2\uparrow} & u_\uparrow + \tilde{g}_{4\uparrow} & \tilde{g}_{2\perp} & \tilde{g}_{4\perp} \\ \tilde{g}_{4\perp} & \tilde{g}_{2\perp} & u_\downarrow + \tilde{g}_{4\downarrow} & \tilde{g}_{2\downarrow} \\ \tilde{g}_{2\perp} & \tilde{g}_{4\perp} & \tilde{g}_{2\downarrow} & u_\downarrow + \tilde{g}_{4\downarrow} \end{pmatrix}, \qquad (14)$$

and $\tilde{g}_{i\lambda,\perp} = g_{i\lambda,\perp}/(2\pi)$.

We show in Appendix A that the matrix $\hat{\mathcal{H}}$ can be brought to the form

$$\hat{\mathcal{H}} = \sum_{P,\nu} u_\nu \boldsymbol{\omega}_{P\nu} (\boldsymbol{\omega}_{P\nu})^T, \qquad (15)$$

with real vectors $\boldsymbol{\omega}_{P\nu}$ satisfying the orthonormal conditions

$$(\boldsymbol{\omega}_{P\nu})^T \hat{C} \boldsymbol{\omega}_{P'\nu'} = s_P \delta_{PP'} \delta_{\nu\nu'}. \qquad (16)$$

Here the subscript ν takes two possible values, which we will denote as c and s, parameters u_c and u_s are positive, and the matrix $\hat{C}$ is defined as $\hat{C} = \text{diag}(1, -1, 1, -1)$ and accounts for the sign factor s_P in the commutation relations (9).

We then introduce chiral fields

$$\tilde{\varphi}_{P\nu}(x) = (\boldsymbol{\omega}_{P\nu})^T \boldsymbol{\varphi}(x), \qquad (17)$$

satisfying the same commutation relations as the original fields $\varphi_{P\lambda}$ [see Eq. (9)]. In terms of these new fields the Hamiltonian (13) takes the simple form

$$\tilde{\mathcal{H}} = \frac{\hbar}{4\pi} \sum_{\nu=c,s} u_\nu \{[\partial_x \tilde{\varphi}_{R\nu}(x)]^2 + [\partial_x \tilde{\varphi}_{L\nu}(x)]^2\}. \qquad (18)$$

The positive constants u_c and u_s have the meanings of the velocities of the two types of elementary excitations of the Hamiltonian $\tilde{\mathcal{H}}$. We refer to these excitations as the holons and spinons. We then introduce the fields

$$\tilde{\phi}_\nu = \tfrac{1}{2}(\tilde{\varphi}_{L\nu} + \tilde{\varphi}_{R\nu}), \quad \tilde{\Pi}_\nu = \frac{1}{2\pi} \partial_x(\tilde{\varphi}_{L\nu} - \tilde{\varphi}_{R\nu}), \qquad (19)$$

and rewrite the effective Hamiltonian density as

$$\tilde{\mathcal{H}} = \frac{\hbar}{2\pi} \sum_{\nu=c,s} u_\nu [\pi^2 \tilde{\Pi}_\nu^2 + (\partial_x \tilde{\phi}_\nu)^2]. \qquad (20)$$

Hence the system of 1D interacting electrons in a magnetic field can be described as a two-component TL liquid.[12] We note that at $B=0$ the holon and spinon modes reduce to the charge and spin modes in Eqs. (3) and (4), respectively.

The fields $\tilde{\phi}_\nu$ and $\tilde{\Pi}_\nu$ are related to the original bosonic fields

$$\phi_\lambda = \tfrac{1}{2}(\varphi_{L\lambda} + \varphi_{R\lambda}), \quad \Pi_\lambda = \frac{1}{2\pi} \partial_x(\varphi_{L\lambda} - \varphi_{R\lambda}) \qquad (21)$$

used in the Hamiltonian (3) and (4) through Eqs. (17) and (19). Due to the parity symmetry of the system, this linear relation is simplified to

$$\begin{pmatrix} \phi_\uparrow \\ \phi_\downarrow \end{pmatrix} = \hat{A}^T \begin{pmatrix} \tilde{\phi}_c \\ \tilde{\phi}_s \end{pmatrix}, \quad \begin{pmatrix} \Pi_\uparrow \\ \Pi_\downarrow \end{pmatrix} = \hat{A}^{-1} \begin{pmatrix} \tilde{\Pi}_c \\ \tilde{\Pi}_s \end{pmatrix}, \qquad (22)$$

where the real matrix $\hat{A}$ can be obtained from the vectors $\boldsymbol{\omega}_{P\nu}$ (see Appendix B). Note that our Hamiltonian (20) is determined by six parameters: the velocities of holons and spinons u_c and u_s, as well as the four elements of the transformation matrix $\hat{A}$.

An alternative approach to the bosonized description of 1D systems in magnetic field was used in Ref. 14. In their theory the Hamiltonian depends on five parameters, namely the velocities u_ρ and u_σ of the charge and spin modes in the absence of the field, the TL-liquid parameters K_ρ and K_σ, and the difference of velocities of spin-$\uparrow$ and spin-$\downarrow$ electrons induced by the field. (In the realistic case of spin-independent interactions between electrons, $K_\sigma = 1$, and the number of parameters is further reduced to four.) This simplification of the theory[14] occurred because the magnetic field dependence of the coupling constants describing the electron-electron interactions was neglected. We believe the approach of Ref. 14 is therefore inapplicable beyond the regime of weak magnetic field.

B. One-dimensional Hubbard model

The effective Hamiltonian (20) depends on six parameters, u_c, u_s, and the four matrix elements of $\hat{A}$. In the case of exactly solvable models, these parameters can be obtained exactly by solving the integral equations of the Bethe ansatz.[10,11] Here we discuss one such case, namely the 1D Hubbard model.

The original Hamiltonian of the 1D Hubbard model has the form

$$H_{\text{Hub}} = -t \sum_{l,\lambda} (c_{l,\lambda}^\dagger c_{l+1,\lambda} + \text{H.c.}) + U \sum_l n_{l,\uparrow} n_{l,\downarrow}$$

$$- \frac{B}{2} \sum_l (n_{l,\uparrow} - n_{l,\downarrow}), \qquad (23)$$

where $c_{l,\lambda}^\dagger$ ($c_{l,\lambda}$) is the creation (annihilation) operator of spin-λ electron at the lth site, $n_{l,\lambda} = c_{l,\lambda}^\dagger c_{l,\lambda}$, the matrix element t accounts for hopping between neighboring lattice sites, and U is the strength of the on-site repulsion; $t, U > 0$. Throughout this paper, we concentrate on the case of less than half-filling, i.e., the total electron density $n < 1$. We will comment on the case of $n > 1$ in Sec. IV.

The 1D Hubbard model allows for exact solution by Bethe ansatz at an arbitrary value of the field B. This solution enables one to obtain not only the velocities u_c and u_s, but also the asymptotics of various correlation functions at large distances. The latter are expressed in terms of the so-called

dressed charges $Z_{\nu\nu'}$, which can be found exactly by solving integral equations of the Bethe ansatz.[10,11] For example, the dressed charge matrix is given by

$$\begin{pmatrix} Z_{cc} & Z_{cs} \\ Z_{sc} & Z_{ss} \end{pmatrix} = \begin{pmatrix} \xi & 0 \\ \frac{1}{2}\xi & 1/\sqrt{2} \end{pmatrix} \quad (24)$$

at $B=0$, and

$$\begin{pmatrix} Z_{cc} & Z_{cs} \\ Z_{sc} & Z_{ss} \end{pmatrix} = \begin{pmatrix} 1 & \dfrac{2}{\pi}\arctan\left(\dfrac{4t\sin(\pi n)}{U}\right) \\ 0 & 1 \end{pmatrix} \quad (25)$$

in the saturation limit where the electron spins are fully polarized. Here the dressed charge ξ is defined in Eq. (5.1) in Ref. 10 and takes values in the range $1 \leq \xi \leq \sqrt{2}$. As the magnetization increases, the dressed charges change continuously between the values in the limiting cases.

By comparing the critical exponents obtained from the Bethe ansatz with those from the effective Hamiltonian (20), one can relate the matrix $\hat{A}$ to the dressed charges $Z_{\nu\nu'}$ as[12,15]

$$\hat{A} = \begin{pmatrix} A_{11} & A_{12} \\ A_{21} & A_{22} \end{pmatrix} = \begin{pmatrix} Z_{cc} - Z_{sc} & Z_{sc} \\ Z_{ss} - Z_{cs} & -Z_{ss} \end{pmatrix}. \quad (26)$$

We will use these results in Sec. III.

As a simple model for an impurity potential in the Hubbard model, we can take the on-site potential

$$V_{\text{Hub}} = V_0(n_{0,\uparrow} + n_{0,\downarrow}). \quad (27)$$

To analyze low-energy transport properties, we take the continuum limit, where the density operator is approximated as $n_{0,\lambda} \approx \Psi_\lambda^\dagger(0)\Psi_\lambda(0)$. With the chiral electron fields the potential is further reduced to the form $V = V_\uparrow + V_\downarrow$, where

$$V_\lambda = v_\lambda[\Psi_{R\lambda}^\dagger(0)\Psi_{L\lambda}(0) + \Psi_{L\lambda}^\dagger(0)\Psi_{R\lambda}(0)]. \quad (28)$$

Here we have kept only the backward scattering terms and discarded the forward scattering ones, as the latter do not affect the conductance. We have also introduced spin-dependent backscattering amplitude v_λ. Finally, Eq. (28) is written in terms of the bosonic fields as

$$V_\lambda = -\frac{v_\lambda}{\pi a} \cos[2\phi_\lambda(x=0)]. \quad (29)$$

We set the amplitudes v_λ to be positive, which is always possible by the transformation $\phi_\lambda \to \phi_\lambda + \text{const}$.

C. Quantum wires at low electron density

Here we derive the low-energy effective Hamiltonian of a quantum wire in the low-density limit, where the effective Hamiltonian (20) takes a particularly simple form similar to Eqs. (3) and (4), as we will see below.

When the electron density in the wire is very low, the electron-electron interactions are effectively very strong. In the limit of infinitely strong repulsion, electrons can never occupy the same position in space and can be viewed as distinguishable particles. As a result, the energy of the elec-

tron system becomes independent of the electron spins. At strong but finite interactions, the electrons in the wire can exchange their positions, and the spins of neighboring electrons are weakly coupled to each other. The resulting spin dynamics is described by the Heisenberg model,

$$H_\sigma = J\sum_l \mathbf{S}_l \cdot \mathbf{S}_{l+1}. \quad (30)$$

Hence the Hamiltonian of the wire at zero magnetic field $B=0$ takes the spin-charge separated form[16,17] $H = H_\rho + H_\sigma$ with the two terms given by Eqs. (3) and (30).

At energy scales below the exchange constant J the Hamiltonian (30) can be bosonized,[7,8] and the form (4) of the Hamiltonian density $\mathcal{H}_\sigma$ is recovered. The advantage of using the Heisenberg form (30) is that the magnetic field B can be easily incorporated by adding a term $-|g|\mu_B B S^z$, where g is Lande factor and μ_B is Bohr magneton. The field B polarizes the spins and results in finite magnetization.[18] In the following, it will be convenient to parametrize the Hamiltonian by a relative magnetization m defined as $m = (n_\uparrow - n_\downarrow)/(n_\uparrow + n_\downarrow)$, where $n_{\uparrow,\downarrow}$ are the densities of electrons with given spin components. At $m < 1$ the Hamiltonian of the Heisenberg model in a magnetic field can be bosonized to the form (4), with the velocity u_σ and the coupling parameter K_σ becoming functions of m.[19] As m varies from 0 to 1, the velocity $u_\sigma(m)$ changes from $\pi J/[2\hbar(n_\uparrow+n_\downarrow)]$ to zero, and $K_\sigma(m)$ grows from 1 to 2.

Using the separation of charge and spin variables in the form (3) and (30), and the above-mentioned properties of the Heisenberg model, one can conclude that the low-energy Hamiltonian density of a strongly interacting electron system in a magnetic field has the form

$$\widetilde{\mathcal{H}} = \frac{\hbar u_\rho}{2}\left[\pi K_\rho(\Pi_\rho + m\Pi_\sigma)^2 + \frac{1}{\pi K_\rho}(\partial_x\phi_\rho)^2\right]$$
$$+ \frac{\hbar u_\sigma(m)}{2}\left[\pi K_\sigma(m)\Pi_\sigma^2 + \frac{[\partial_x(\phi_\sigma - m\phi_\rho)]^2}{\pi K_\sigma(m)}\right]. \quad (31)$$

The first line of the Hamiltonian (31) describes the charge density excitations (holons) of the electron system. Since the coupling of the spins is very weak, the magnetic field polarizing the spins does not affect the speed of holons u_ρ. The form of the holon part is thus essentially equivalent to Eq. (3), with the addition of the term $m\Pi_\sigma$ to the momentum density. This correction does not affect the dynamics of the holons, as $[\Pi_\sigma, \partial_x\phi_\rho] = 0$. On the other hand, the addition of $m\Pi_\sigma$ to the momentum density ensures that the holon wave carries the spin current due to the finite magnetization m of the ground state. Indeed, the equation of motion for the holon wave results in the relation $\dot{\phi}_\sigma = m\dot{\phi}_\rho$ between the spin and charge currents.

The form of the spinon part of the Hamiltonian essentially reproduces the bosonized Hamiltonian of the Heisenberg model at finite magnetization; in particular, the dependences $u_\sigma(m)$ and $K_\sigma(m)$ are equivalent to those discussed in Ref. 19. The only difference is the addition of the term $-m\partial_x\phi_\rho$ to the spin density. Due to the commutation relation $[\phi_\rho, \Pi_\sigma] = 0$, this term does not change the spin dynamics. However,

its presence ensures that in the spinon ground state the spin and charge densities are proportional to each other: $\partial_x \phi_\sigma = m \partial_x \phi_\rho$.

The effective Hamiltonian (31) can be easily brought to the standard form (20), with the matrix $\hat{A}$ taking the form

$$
\hat{A} = \begin{pmatrix} A_{11} & A_{12} \\ A_{21} & A_{22} \end{pmatrix} = \begin{pmatrix} \sqrt{\dfrac{K_\rho}{2}}(1+m) & \sqrt{\dfrac{K_\rho}{2}}(1-m) \\ \sqrt{\dfrac{K_\sigma(m)}{2}} & -\sqrt{\dfrac{K_\sigma(m)}{2}} \end{pmatrix}.
$$

(32)

In general, the parameter K_ρ is nonuniversal. In the limit of strong short-range interaction it can be deduced from the well-known properties of the Hubbard model, and one finds $K_\rho = \frac{1}{2}$. For longer range interactions one expects $K_\rho < \frac{1}{2}$. On the other hand, the parameter $K_\sigma(m)$ is the TL-liquid parameter for the Heisenberg spin chain in magnetic field, which can be determined exactly by solving the Bethe ansatz integral equations.[19,20] These results will be used in Sec. III to investigate the renormalizations of impurity potential.

Our discussion in this section assumed an arbitrary range of interactions between the electrons in the quantum wire. In experiments the range of the Coulomb repulsion between electrons is usually longer than the distance between particles. However, the range of the interactions is limited by the presence of metal gates in the vicinity of the wire. One can show that at electron densities below a_B/d^2 the range of the interactions is short compared with the distance between the electrons.[17] (Here d is the distance from the wire to the nearest gate, and a_B is the effective Bohr radius in the material; $a_B \approx 10$ nm in GaAs.) In this special case the electrons in the quantum wire can be described[17] by the Hubbard model in the limit of low filling, $n \to 0$, when the discreteness of the lattice can be neglected. In particular, the fact that the spin excitations are those of the Heisenberg model (30) corresponds to the well-known property[21] of the Hubbard model in the limit $U/t \to \infty$. In this limit the parameter K_ρ takes the value $\frac{1}{2}$. We have checked that at $K_\rho = \frac{1}{2}$ our result (32) for the matrix $\hat{A}$ coincides with the result (26) for the Hubbard model with the dressed charges $Z_{\nu\nu'}$ found in the limit $U/t \to \infty$ in Ref. 22.

Similarly to the case of the Hubbard model, the presence of an impurity in a quantum wire results in backscattering of electrons. We will use expressions (28) and (29) for the perturbations in the Hamiltonian, cf. Refs. 1 and 2.

III. RENORMALIZATION-GROUP ANALYSIS

In this section we discuss the renormalizations of impurity backscattering amplitude v_λ and tunneling amplitude t_λ using the effective Hamiltonian obtained in Sec. II. We will consider the following four limiting cases:

$$|v_\uparrow| \ll D \text{ and } |v_\downarrow| \ll D, \tag{33a}$$

$$|t_\uparrow| \ll D \text{ and } |t_\downarrow| \ll D, \tag{33b}$$

$$|v_\uparrow| \ll D \text{ and } |t_\downarrow| \ll D, \tag{33c}$$

TABLE I. The scaling dimensions of the backscattering and tunneling operators V_λ and T_λ in the four limiting cases (33a)–(33d). The expressions of $x_{V\lambda}$ and $x_{T\lambda}$ are given in Eqs. (40) and (45), respectively.

Limits	$V_\uparrow$	$V_\downarrow$	$T_\uparrow$	$T_\downarrow$
(a) $\|v_\uparrow\|, \|v_\downarrow\| \ll D$	$x_{V\uparrow}$	$x_{V\downarrow}$	$\cdots$	$\cdots$
(b) $\|t_\uparrow\|, \|t_\downarrow\| \ll D$	$\cdots$	$\cdots$	$x_{T\uparrow}$	$x_{T\downarrow}$
(c) $\|v_\uparrow\|, \|t_\downarrow\| \ll D$	$1/x_{T\uparrow}$	$\cdots$	$\cdots$	$1/x_{V\downarrow}$
(d) $\|t_\uparrow\|, \|v_\downarrow\| \ll D$	$\cdots$	$1/x_{T\downarrow}$	$1/x_{V\uparrow}$	$\cdots$

$$|t_\uparrow| \ll D \text{ and } |v_\downarrow| \ll D. \tag{33d}$$

Scaling dimensions of the backscattering and tunneling operators in the four cases are summarized in Table I. Evaluating the scaling dimensions quantitatively, we construct the RG flow diagram in the $v_\uparrow$-$v_\downarrow$ plane. We will see that the RG flow diagram changes drastically when a sufficiently strong field is applied.

A. Scaling dimensions of backscattering and tunneling operators

1. Weak-potential limit $|v_\uparrow|, |v_\downarrow| \ll D$

First, we discuss the renormalization of the impurity scattering in the limit where both $v_\uparrow$ and $v_\downarrow$ are weak, $|v_\uparrow|, |v_\downarrow| \ll D$. To find the scaling dimension of the operator (29), we calculate the ground-state correlation function of V_λ using the action for the pure system (20) given by

$$
S = \sum_{\nu=c,s} \int_0^\beta d\tau \int_{-\infty}^\infty dx \left(\frac{1}{2\pi u_\nu} [\partial_\tau \tilde{\phi}_\nu(x,\tau)]^2 + \frac{u_\nu}{2\pi} [\partial_x \tilde{\phi}_\nu(x,\tau)]^2 \right),
$$

(34)

where $\beta = 1/T$ and τ is the imaginary time. Since V_λ depends only on $\phi_\lambda^0(\tau) \equiv \phi_\lambda(x=0,\tau)$, we integrate out the fields $\tilde{\phi}_\nu(x,\tau)$ at $x \neq 0$ to derive the effective action for $\tilde{\phi}_\nu(x=0,\tau)$,

$$
S_0 = \sum_{\omega_n} \frac{|\omega_n|}{\pi} (|\tilde{\phi}_c^0(\omega_n)|^2 + |\tilde{\phi}_s^0(\omega_n)|^2). \tag{35}
$$

Here we have introduced the Fourier transform

$$
\tilde{\phi}_\nu^0(\omega_n) = \frac{1}{\sqrt{\beta}} \int_0^\beta e^{i\omega_n \tau} \tilde{\phi}_\nu(x=0,\tau) d\tau \tag{36}
$$

with $\omega_n = 2\pi n/\beta$. Using the effective action, the imaginary-time correlation function is calculated as

$$
\langle e^{2i\phi_\lambda^0(\tau)} e^{-2i\phi_\lambda^0(0)} \rangle = \frac{1}{Z} \int \mathcal{D}\tilde{\phi}_c^0 \mathcal{D}\tilde{\phi}_s^0 e^{-S_0 + 2i[\phi_\lambda^0(\tau) - \phi_\lambda^0(0)]},
$$

(37)

where

$$Z = \int \mathcal{D}\tilde{\phi}_c^0 \mathcal{D}\tilde{\phi}_s^0 e^{-S_0} \tag{38}$$

is the partition function. A straightforward calculation of Eq. (37) with Eqs. (35) and (22) gives the correlation functions in the limit $\beta \to \infty$,

$$\langle V_\lambda(\tau)V_\lambda(0)\rangle \propto \tau^{-2x_{V\lambda}}, \tag{39}$$

with the scaling dimensions $x_{V\lambda}$ given by

$$x_{V\uparrow} = A_{11}^2 + A_{21}^2, \tag{40a}$$

$$x_{V\downarrow} = A_{12}^2 + A_{22}^2. \tag{40b}$$

The exponents α_λ in Eq. (1) in this limit are given by

$$\alpha_\lambda^{(a)} = x_{V\lambda} - 1. \tag{41}$$

2. Weak-tunneling limit $|t_\uparrow|, |t_\downarrow| \ll D$

The renormalizations of tunneling through a strong impurity potential were studied using several different approaches.[1,2,23] The discussion given below uses the method of Ref. 23.

Let us consider the tunneling of a spin-$\uparrow$ electron through the impurity potential at $x = 0$. Since the potential amplitudes v_λ ($\lambda = \uparrow, \downarrow$) are assumed to be very large, the fields ϕ_λ^0 are pinned at the minima of the potential V_λ [Eq. (29)], i.e., $\phi_\lambda^0 = \pi l_\lambda$, where l_λ are integers. The tunneling of a spin-$\uparrow$ electron through the potential barrier is equivalent to a sudden change of $\phi_\uparrow^0$ between neighboring minima, say, from $\phi_\uparrow^0 = 0$ to $\phi_\uparrow^0 = \pi$, i.e., a jump in $\phi_\uparrow^0$ by π. Let us denote the operator for this tunneling process by $T_\uparrow$. The correlation function $\langle T_\uparrow^\dagger(\tau)T_\uparrow(0)\rangle$ is then obtained from

$$\langle T_\uparrow^\dagger(\tau)T_\uparrow(0)\rangle \propto \exp(-S_0)\big|_{\phi_\uparrow^0(\tau') = \pi\theta(\tau'-\tau), \phi_\downarrow^0 = 0}, \tag{42}$$

where we have ignored small fluctuations of ϕ_λ^0 around the potential minima. [Here $\theta(\tau)$ is the unit step function.] From Eq. (22) we substitute

$$\begin{pmatrix} \tilde{\phi}_c^0(\omega_n) \\ \tilde{\phi}_s^0(\omega_n) \end{pmatrix} = (\hat{A}^T)^{-1}\begin{pmatrix} i\pi(1 - e^{i\omega_n\tau})/\omega_n\sqrt{\beta} \\ 0 \end{pmatrix} \tag{43}$$

into $\exp(-S_0)$ to find

$$\langle T_\uparrow^\dagger(\tau)T_\uparrow(0)\rangle \propto \tau^{-2x_{T\uparrow}}, \tag{44}$$

where the scaling dimension is

$$x_{T\uparrow} = [(A^{-1})_{11}]^2 + [(A^{-1})_{12}]^2 = \frac{A_{22}^2 + A_{12}^2}{(\det\hat{A})^2}. \tag{45a}$$

Similarly we have

$$x_{T\downarrow} = [(A^{-1})_{21}]^2 + [(A^{-1})_{22}]^2 = \frac{A_{21}^2 + A_{11}^2}{(\det\hat{A})^2}. \tag{45b}$$

The exponents for the tunneling amplitude t_λ in Eq. (1) in this limit are

$$\beta_\lambda^{(b)} = x_{T\lambda} - 1. \tag{46}$$

3. Asymmetric limits $|v_\uparrow|, |t_\downarrow| \ll D$ and $|t_\uparrow|, |v_\downarrow| \ll D$

Next we consider the asymmetric limit where the potential scattering is weak for the spin-$\uparrow$ electrons but strong for the spin-$\downarrow$ electrons. Although such an extremely spin-selective scattering is not likely to be realized with a bare impurity potential, we will see in Sec. III B that this is indeed realized for some RG trajectory if a magnetic field applied is sufficiently large.

The scaling dimension of the potential $V_\uparrow$ in the limit $|v_\uparrow|, |t_\downarrow| \ll D$ can be found in a similar way to the weak potential limit discussed in Sec. III A 1. The only difference is that in the present case $\phi_\downarrow(x=0)$ is pinned at a potential minimum $\pi l_\downarrow$ by the strong impurity potential $V_\downarrow$. The asymptotic form of the ground-state correlation function is then obtained as

$$\langle V_\uparrow(\tau)V_\uparrow(0)\rangle \propto \int \mathcal{D}\phi_\uparrow^0 e^{-S_0 + 2i[\phi_\uparrow^0(\tau) - \phi_\uparrow^0(0)]}\bigg|_{\phi_\downarrow^0 = 0} \propto \tau^{-2/x_{T\uparrow}}, \tag{47}$$

with $x_{T\uparrow}$ given by Eq. (45a). Therefore the scaling dimension of $V_\uparrow$ in this limit is $1/x_{T\uparrow}$, and the exponent $\alpha_\uparrow$ is given by

$$\alpha_\uparrow^{(c)} = \frac{1}{x_{T\uparrow}} - 1. \tag{48}$$

Similarly, the scaling dimension of $V_\downarrow$ in the limit $|t_\uparrow|, |v_\downarrow| \ll D$ is found to be $1/x_{T\downarrow}$, resulting in the exponent $\alpha_\downarrow^{(d)} = 1/x_{T\downarrow} - 1$.

The scaling of the tunneling operator $T_\uparrow$ in the limit $|t_\uparrow|, |v_\downarrow| \ll D$ can be studied in a similar manner to that in Sec. III A 2. In the present case, however, the potential $V_\downarrow$ is weak, and the field $\phi_\downarrow^0$ can fluctuate almost freely. Therefore, to find the scaling dimension in lowest order in $v_\downarrow$, we first integrate out $\phi_\downarrow^0$ in S_0 to obtain the effective action for $\phi_\uparrow^0$, into which we substitute $\phi_\uparrow^0(\tau') = \pi\theta(\tau' - \tau)$. This yields

$$\langle T_\uparrow^\dagger(\tau)T_\uparrow(0)\rangle \propto \int \mathcal{D}\phi_\downarrow^0 e^{-S_0}\bigg|_{\phi_\uparrow^0(\tau') = \pi\theta(\tau'-\tau)} \propto \tau^{-2/x_{V\uparrow}}, \tag{49}$$

with $x_{V\uparrow}$ given by Eq. (40a). We thus conclude that the scaling dimension of $T_\uparrow$ in the limit (33d) is $1/x_{V\uparrow}$, and the exponent $\beta_\uparrow^{(d)} = 1/x_{V\uparrow} - 1$. Similarly, the scaling dimension of $T_\downarrow$ in the limit (33c) is $1/x_{V\downarrow}$, and the exponent $\beta_\downarrow^{(c)} = 1/x_{V\downarrow} - 1$.

B. RG flow diagram

In the preceding sections we have found that the scaling dimensions of the backscattering and tunneling operators in the four limits (33a)–(33d) are given in terms of the matrix elements of $\hat{A}$. We thus need to compute these matrix elements to determine whether the perturbing operators in each limit are relevant or irrelevant. As we have seen in Sec. II, this can be achieved for electron systems with short-range interactions, i.e., the Hubbard chain at less than half-filling, and the quantum wire in the low electron-density limit. The dressed charges $Z_{\nu\nu'}$ for the former case and the parameter
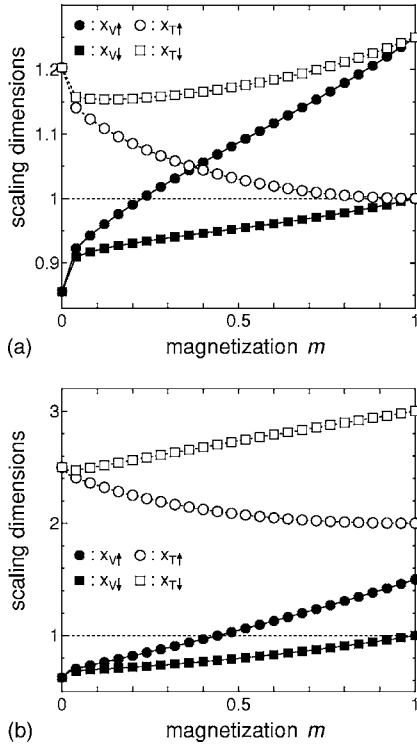
FIG. 1. The magnetization dependence of scaling dimensions $x_{V\lambda}$ and $x_{T\lambda}$, computed from the Bethe ansatz integral equations (a) for the Hubbard chain with $U/t=4$ and $n=0.5$ and (b) for the quantum wire with $K_\rho=\frac{1}{4}$ in the low-density limit.

$K_\sigma(m)$ for the latter one can be calculated as functions of m by solving the corresponding Bethe ansatz integral equations. We have solved the integral equations numerically, and the results are discussed below. The readers who are interested in the details of the Bethe ansatz analysis should refer to Refs. 10 and 11 for the Hubbard chain and Ref. 20 for the Heisenberg chain.

In Fig. 1 we plot the scaling dimensions $x_{V\lambda}$ and $x_{T\lambda}$ obtained numerically for the Hubbard chain at $n<1$ and the low-density quantum wire as functions of the relative magnetization m. The two systems exhibit qualitatively the same behavior. At zero magnetization $m=0$, we see that $x_{V\uparrow}=x_{V\downarrow}<1$ and $x_{T\uparrow}=x_{T\downarrow}>1$. This is in accordance with the well-known scaling behavior in SU(2) symmetric systems, $\alpha_\uparrow^{(a)}$

$=\alpha_\downarrow^{(a)}<0$ and $\beta_\uparrow^{(b)}=\beta_\downarrow^{(b)}>0$. The dimensions $x_{V\uparrow}$ and $x_{V\downarrow}$ increase with m. In the limit of full spin polarization $m\to 1$ the dimension $x_{V\uparrow}$ reaches a certain value y greater than 1, whereas $x_{V\downarrow}\to 1$. (In the Hubbard model $x_{T\downarrow}$ and $x_{T\uparrow}$ also approach y and 1 as $m\to 1$.) The most important point here is that the dimension $x_{V\uparrow}$ exceeds 1 for m larger than certain critical magnetization m_c. This implies that the exponents $\alpha_\uparrow^{(a)}$ and $\beta_\uparrow^{(d)}$ change their sign at $m=m_c$, and the direction of the RG flows reverses. The significance of this effect can be quantified by the value of y, which is given by $y=1+\{1-(2/\pi)\arctan[4t\sin(\pi n)/U]\}^2$ for the Hubbard chain at $n<1$ and $y=1+2K_\rho$ for the quantum wire in the low electron-density limit. On the other hand, the dimensions $x_{T\uparrow}$ and $x_{T\downarrow}$ are larger than 1 at any m, indicating that the scaling of the operators related to them does not change qualitatively between $m>m_c$ and $m<m_c$. We have checked that the dependence of the scaling dimensions on the magnetization m remains qualitatively the same regardless of the interaction strength U/t and the electron density $n<1$ in the Hubbard model, or the exact value of $K_\rho<\frac{1}{2}$ for low-density quantum wires.

From the magnetization dependence of the scaling dimensions $x_{V\lambda}$ and $x_{T\lambda}$ discussed above, we can deduce the RG flow diagram of $(v_\uparrow,v_\downarrow)$ as shown in Fig. 2. When the magnetization is small, $m<m_c$, the backscattering of electrons by an impurity is enhanced by repulsive interactions. As a result, the RG trajectories go directly to the strong-backscattering fixed point $(v_\uparrow,v_\downarrow)=(\infty,\infty)$ [Figs. 2(a) and 2(b)]. The magnetic field bends the RG trajectories upward but does not change the essential features of the renormalization flow.

On the other hand, when the applied field is sufficiently strong to achieve $m>m_c$, the backscattering operator $V_\uparrow$ of spin-$\uparrow$ electrons becomes irrelevant in the weak-potential limit. That is, the electron-electron interactions *suppress* the backscattering of majority-spin electrons by a weak impurity. As a result, the RG trajectories in the vicinity of $(v_\uparrow,v_\downarrow)=(0,0)$ flow toward the line $v_\uparrow=0$ [Fig. 2(c)]. Thus, if the bare backscattering amplitudes are not too large, they are renormalized toward the asymmetric limit $(v_\uparrow,v_\downarrow)=(0,\infty)$. This means that, in a certain regime of RG transformations or, equivalently, at certain energy and temperature range, a situation is realized where the impurity potential becomes almost transparent for majority-spin electrons but almost im-
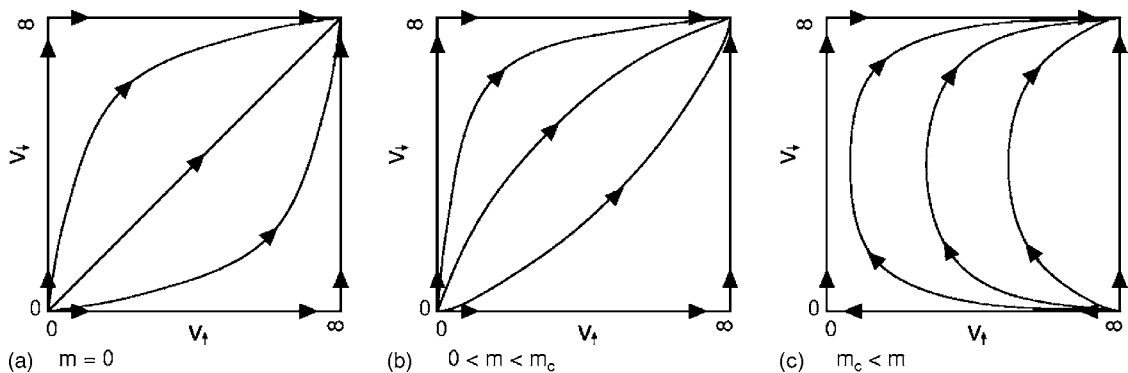

FIG. 2. The schematic RG flow diagram for (a) $m=0$, (b) $0<m<m_c$, and (c) $m>m_c$.

penetrable for minority-spin electrons. However, since the asymmetric fixed point $(v_\uparrow, v_\downarrow) = (0, \infty)$ is unstable, the potentials are eventually renormalized to the strong-scattering fixed point $(v_\uparrow, v_\downarrow) = (\infty, \infty)$, with decreasing energy scale or temperature $T \to 0$. In this sense, a weak impurity potential can have a spin-filtering effect generating a spin-polarized current.

IV. SUMMARY

In this paper we have studied the effect of magnetic field on the RG flow of a single impurity potential in 1D interacting electron systems. Within the Abelian bosonization theory, the low-energy physics of the system is described as a Gaussian model with two independent modes of bosonic excitations. The coupling parameters A_{ij} are obtained from the Bethe ansatz for the 1D Hubbard model at less than half-filling as well as for a quantum wire at the low electron density limit. Using these results, we have evaluated the scaling dimensions of the impurity potential and tunneling operators, and determined the RG flow of the potential amplitudes near the fixed points. We have found that the magnetic field can cause a drastic change in the RG flow diagram. While in a weak field the repulsive interactions always enhance electron backscattering by impurities, in a sufficiently strong field this effect is reduced, and the backscattering of majority-spin electrons by a weak-impurity potential may even be suppressed by the interactions. This means that if the amplitude of the bare potential is small, a spin-filtering phenomenon, in which only the majority-spin electrons can transmit through the renormalized potential, can be realized in a certain temperature regime in the RG flow.

So far we have assumed that the band is less than half filled, $n < 1$. The results obtained at $n < 1$ can be easily translated to the case $n > 1$ by performing the particle-hole transformation, $n_\lambda \to 1 - n_\lambda$. Suppose that the band is more than half-filled and partially spin polarized, $0 < m < 1$. Then, it is the majority-spin holes, i.e., the spin-$\downarrow$ holes, whose backscattering is suppressed in strong magnetic field. In other words, transport of charge carriers of majority-spin is enhanced by interactions.

The renormalizations of the impurity potential in the presence of magnetic field have also been considered in a recent preprint.[24,25] Although the authors of Ref. 24 also found the regime in which the weak backscattering of the majority-spin electrons is suppressed by the interactions, their results differ significantly from ours. Most importantly, in Ref. 24 this interesting regime occurs either in the presence of spin-dependent interactions between electrons or when the interactions are attractive. Both of these regimes are unlikely to be realized in realistic experiments. In contrast to our work, the theory[24] was based upon the treatment of 1D electron systems in magnetic field developed in Ref. 14. As we mentioned in Sec. II A, the latter approach assumes weak magnetic field, i.e., small relative magnetization $m \ll 1$. In contrast, our effect of suppression of weak impurities by interactions occurs at sufficiently strong field, when $m \gtrsim m_c \gtrsim 0.2$ (see Fig. 1), and is expected in the realistic case of spin-independent repulsive interactions.

APPENDIX A: GENERALIZED EIGENVALUE PROBLEM OF $\hat{\mathcal{H}}\hat{C}$

In this Appendix we show how the matrix (14) can be brought to the diagonal form (15). Suppose that $\boldsymbol{\omega}_j$ and $\boldsymbol{\eta}_j$ are the right and left eigenvectors of $\hat{\mathcal{H}}\hat{C}$, respectively, i.e.,

$$\hat{\mathcal{H}}\hat{C}\boldsymbol{\omega}_j = u_j \boldsymbol{\omega}_j, \tag{A1}$$

$$(\boldsymbol{\eta}_j)^T \hat{\mathcal{H}}\hat{C} = u_j (\boldsymbol{\eta}_j)^T. \tag{A2}$$

Then, the matrix $\hat{\mathcal{H}}\hat{C}$ is given by

$$\hat{\mathcal{H}}\hat{C} = \sum_j \boldsymbol{\omega}_j u_j (\boldsymbol{\eta}_j)^T, \tag{A3}$$

where $\boldsymbol{\omega}_j$ and $\boldsymbol{\eta}_j$ obey the biorthogonal condition,

$$(\boldsymbol{\eta}_j)^T \boldsymbol{\omega}_{j'} = \delta_{jj'}. \tag{A4}$$

Since both $\hat{\mathcal{H}}$ and $\hat{C}$ are symmetric, i.e., $(\hat{\mathcal{H}})^T = \hat{\mathcal{H}}$ and $(\hat{C})^T = \hat{C}$, Eq. (A2) can be rewritten as

$$(\hat{\mathcal{H}}\hat{C})^T \boldsymbol{\eta}_j = \hat{C}\hat{\mathcal{H}}\boldsymbol{\eta}_j = u_j \boldsymbol{\eta}_j.$$

Hence, $\boldsymbol{\eta}_j$ satisfies the relation

$$\hat{\mathcal{H}}\hat{C}\hat{C}\boldsymbol{\eta}_j = \hat{C}^2 \hat{\mathcal{H}}\hat{C}^2 \boldsymbol{\eta}_j = \hat{C}\hat{C}\hat{\mathcal{H}}\boldsymbol{\eta}_j = u_j \hat{C}\boldsymbol{\eta}_j, \tag{A5}$$

where we used $\hat{C}^2 = \hat{1}$. This means that $\hat{C}\boldsymbol{\eta}_j$ is a *right* eigenvector of $\hat{\mathcal{H}}\hat{C}$ and proportional to $\boldsymbol{\omega}_j$,

$$\boldsymbol{\omega}_j = c_j \hat{C}\boldsymbol{\eta}_j, \tag{A6}$$

where c_j is a constant. Furthermore, assuming that the Hamiltonian matrix $\hat{\mathcal{H}}$ is positive definite,[26] it follows that c_j and u_j have the same sign,

$$(\boldsymbol{\omega}_j)^T \hat{C}\hat{\mathcal{H}}\hat{C}\boldsymbol{\omega}_j = u_j (\boldsymbol{\omega}_j)^T \hat{C}\boldsymbol{\omega}_j = u_j c_j (\boldsymbol{\eta}_j)^T \boldsymbol{\omega}_j = u_j c_j > 0. \tag{A7}$$

We can therefore relate $\boldsymbol{\eta}_j$ to $\boldsymbol{\omega}_j$ as

$$\boldsymbol{\omega}_j = \mathrm{sgn}(u_j)\hat{C}\boldsymbol{\eta}_j \tag{A8}$$

without any loss of generality. Using Eqs. (A3) and (A8), one finds that the right eigenvectors $\boldsymbol{\omega}_j$ satisfy Eq. (15),

$$\hat{\mathcal{H}} = \hat{\mathcal{H}}\hat{C}\hat{C} = \sum_j \boldsymbol{\omega}_j u_j (\boldsymbol{\eta}_j)^T \hat{C} = \sum_j \boldsymbol{\omega}_j u_j (\boldsymbol{\omega}_j)^T \mathrm{sgn}(u_j)$$

$$= \sum_j |u_j| \boldsymbol{\omega}_j (\boldsymbol{\omega}_j)^T.$$

The vectors $\boldsymbol{\omega}_j$ satisfy certain orthonormal conditions, which can be derived as follows. Suppose that $\hat{P}$ is a matrix of parity transformation exchanging the right- and left-moving fields. Due to the parity symmetry of the Hamiltonian, the vectors $\boldsymbol{\omega}_j$ and $\hat{P}\boldsymbol{\omega}_j$ have the following property: if $\boldsymbol{\omega}_j$ is a right eigenvector of $\hat{\mathcal{H}}\hat{C}$ with an eigenvalue u_j, i.e., $\hat{\mathcal{H}}\hat{C}\boldsymbol{\omega}_j = u_j\boldsymbol{\omega}_j$, then $\hat{P}\boldsymbol{\omega}_j$ is another right eigenvector, with eigenvalue $-u_j$,

$$\hat{\mathcal{H}}\hat{C}\hat{P}\boldsymbol{\omega}_j = -\hat{P}\hat{\mathcal{H}}\hat{C}\boldsymbol{\omega}_j = -u_j\hat{P}\boldsymbol{\omega}_j, \tag{A9}$$

where we used the relations $\hat{P}\hat{\mathcal{H}}\hat{P} = \hat{\mathcal{H}}$ and $\hat{P}\hat{C}\hat{P} = -\hat{C}$. Hence, we can classify the vectors $\boldsymbol{\omega}_j$ into two pairs, $\boldsymbol{\omega}_{Pc}$ and $\boldsymbol{\omega}_{Ps}$, where the right and left movers in each pair are related as $\boldsymbol{\omega}_{L\nu} = \hat{P}\boldsymbol{\omega}_{R\nu}$. Using these results and Eqs. (A4) and (A8), we find that the vectors $\boldsymbol{\omega}_{P\nu}$ obey the orthonormal conditions (16).

APPENDIX B: MATRIX $\hat{A}$

Here we outline the diagonalization procedure transforming the Hamiltonian (13) to the form (20) and express matrix $\hat{A}$ in terms of the velocities $u_{\uparrow,\downarrow}$ and the coupling constants $\tilde{g}_{i\lambda,\perp}$.

We denote the elements of the vectors $\boldsymbol{\omega}_{P\nu}$ as

$$\boldsymbol{\omega}_{R\nu} = \begin{pmatrix} a_{\nu\uparrow} \\ b_{\nu\uparrow} \\ a_{\nu\downarrow} \\ b_{\nu\downarrow} \end{pmatrix}, \quad \boldsymbol{\omega}_{L\nu} = \hat{P}\boldsymbol{\omega}_{R\nu} = \begin{pmatrix} b_{\nu\uparrow} \\ a_{\nu\uparrow} \\ b_{\nu\downarrow} \\ a_{\nu\downarrow} \end{pmatrix}. \tag{B1}$$

Due to the parity symmetry of these vectors, the fields ϕ_λ and Π_λ do not mix with each other under the transformation. The relation between $\tilde{\phi}_\nu$ ($\tilde{\Pi}_\nu$) and ϕ_λ (Π_λ) has the form

$$\begin{pmatrix} \tilde{\phi}_c \\ \tilde{\phi}_s \end{pmatrix} = \hat{A}_+ \begin{pmatrix} \phi_\uparrow \\ \phi_\downarrow \end{pmatrix}, \quad \begin{pmatrix} \tilde{\Pi}_c \\ \tilde{\Pi}_s \end{pmatrix} = \hat{A}_- \begin{pmatrix} \Pi_\uparrow \\ \Pi_\downarrow \end{pmatrix}, \tag{B2}$$

where the matrix $\hat{A}_\pm$ is given by

$$\hat{A}_\pm = \begin{pmatrix} A_{\pm c\uparrow} & A_{\pm c\downarrow} \\ A_{\pm s\uparrow} & A_{\pm s\downarrow} \end{pmatrix} \tag{B3}$$

with $A_{\pm\nu\lambda} = a_{\nu\lambda} \pm b_{\nu\lambda}$. Using the orthonormal conditions Eq. (16), one can find that the matrices $\hat{A}_\pm$ are related to each other as $(\hat{A}_+)^T = (\hat{A}_-)^{-1}$. We thereby arrive at Eq. (22) by identifying $\hat{A} = \hat{A}_-$.

From the eigenvalue problem Eq. (A1), the linear equation system for $A_{\pm\nu\lambda}$ is obtained as

$$\begin{pmatrix} 0 & 0 & u_\uparrow + \tilde{g}_{4\uparrow} + \tilde{g}_{2\uparrow} & \tilde{g}_{4\perp} + \tilde{g}_{2\perp} \\ 0 & 0 & \tilde{g}_{4\perp} + \tilde{g}_{2\perp} & u_\downarrow + \tilde{g}_{4\downarrow} + \tilde{g}_{2\downarrow} \\ u_\uparrow + \tilde{g}_{4\uparrow} - \tilde{g}_{2\uparrow} & \tilde{g}_{4\perp} - \tilde{g}_{2\perp} & 0 & 0 \\ \tilde{g}_{4\perp} - \tilde{g}_{2\perp} & u_\downarrow + \tilde{g}_{4\downarrow} - \tilde{g}_{2\downarrow} & 0 & 0 \end{pmatrix} \begin{pmatrix} A_{+\nu\uparrow} \\ A_{+\nu\downarrow} \\ A_{-\nu\uparrow} \\ A_{-\nu\downarrow} \end{pmatrix} = u_\nu \begin{pmatrix} A_{+\nu\uparrow} \\ A_{+\nu\downarrow} \\ A_{-\nu\uparrow} \\ A_{-\nu\downarrow} \end{pmatrix}. \tag{B4}$$

By solving this eigenvalue problem, we obtain analytical expressions for the renormalized velocities u_ν,[26]

$$u_c = \sqrt{\frac{p_\uparrow + p_\downarrow + \sqrt{(p_\uparrow - p_\downarrow)^2 + 4qr}}{2}}, \tag{B5}$$

$$u_s = \sqrt{\frac{p_\uparrow + p_\downarrow - \sqrt{(p_\uparrow - p_\downarrow)^2 + 4qr}}{2}}, \tag{B6}$$

and the elements of $\hat{A}_\pm$,

$$A_{+\nu\uparrow} = \sqrt{\frac{(u_\uparrow + \tilde{g}_{4\uparrow} + \tilde{g}_{2\uparrow})(u_\nu^2 - p_\downarrow) + (\tilde{g}_{4\perp} + \tilde{g}_{2\perp})q}{u_\nu(2u_\nu^2 - p_\uparrow - p_\downarrow)}}, \tag{B7}$$

$$A_{+\nu\downarrow} = \frac{u_\nu^2 - p_\uparrow}{q} A_{+\nu\uparrow}, \tag{B8}$$

$$A_{-\nu\uparrow} = \left(1 + \frac{u_\nu^2 - p_\uparrow}{u_\nu^2 - p_\downarrow}\right)^{-1} \frac{1}{A_{+\nu\uparrow}}, \tag{B9}$$

$$A_{-\nu\downarrow} = \frac{u_\nu^2 - p_\uparrow}{r}\left(1 + \frac{u_\nu^2 - p_\uparrow}{u_\nu^2 - p_\downarrow}\right)^{-1} \frac{1}{A_{+\nu\uparrow}}, \tag{B10}$$

where

$$p_\lambda = (u_\lambda + \tilde{g}_{4\lambda})^2 - \tilde{g}_{2\lambda}^2 + \tilde{g}_{4\perp}^2 - \tilde{g}_{2\perp}^2, \tag{B11}$$

$$q = (u_\uparrow + \tilde{g}_{4\uparrow} + \tilde{g}_{2\uparrow})(\tilde{g}_{4\perp} - \tilde{g}_{2\perp}) + (u_\downarrow + \tilde{g}_{4\downarrow} - \tilde{g}_{2\downarrow})(\tilde{g}_{4\perp} + \tilde{g}_{2\perp}), \tag{B12}$$

$$r = (u_\uparrow + \tilde{g}_{4\uparrow} - \tilde{g}_{2\uparrow})(\tilde{g}_{4\perp} + \tilde{g}_{2\perp}) + (u_\downarrow + \tilde{g}_{4\downarrow} + \tilde{g}_{2\downarrow})(\tilde{g}_{4\perp} - \tilde{g}_{2\perp}). \tag{B13}$$

Substituting Eqs. 6.12–6.17 of Ref. 12 into Eqs. (B5)–(B13), we obtain the expression of matrix $\hat{A}$ for the Hubbard model [Eq. (26)].

*On leave from Duke University, Durham, NC 27708-0305.

[1] C. L. Kane and M. P. A. Fisher, Phys. Rev. B **46**, 15233 (1992).

[2] A. Furusaki and N. Nagaosa, Phys. Rev. B **47**, 4631 (1993).

[3] S. Tarucha, T. Honda, and T. Saku, Solid State Commun. **94**, 413 (1995).

[4] O. M. Auslaender, A. Yacoby, R. de Picciotto, K. W. Baldwin, L. N. Pfeiffer, and K. W. West, Phys. Rev. Lett. **84**, 1764 (2000).

[5] M. Bockrath, D. H. Cobden, J. Lu, A. G. Rinzler, R. E. Smalley, L. Balents, and P. L. McEuen, Nature (London) **397**, 598 (1999).

[6] Z. Yao, H. W. C. Postma, L. Balents, and C. Dekker, Nature (London) **402**, 273 (1999).

[7] H. J. Schulz, G. Cuniberti, and P. Pieri, in *Field Theories for Low-Dimensional Condensed Matter Systems*, edited by G. Morandi *et al.* (Springer-Verlag, New York, 2000).

[8] T. Giamarchi, *Quantum Physics in One Dimension* (Clarendon Press, Oxford, 2003).

[9] E. Wong and I. Affleck, Nucl. Phys. B **417**, 403 (1994).

[10] H. Frahm and V. E. Korepin, Phys. Rev. B **42**, 10553 (1990).

[11] H. Frahm and V. E. Korepin, Phys. Rev. B **43**, 5653 (1991).

[12] K. Penc and J. Sólyom, Phys. Rev. B **47**, 6273 (1993).

[13] J. Sólyom, Adv. Phys. **28**, 201 (1979).

[14] T. Kimura, K. Kuroki, and H. Aoki, Phys. Rev. B **53**, 9572 (1996).

[15] D. C. Cabra, A. De Martino, A. Honecker, P. Pujol, and P. Simon, Phys. Rev. B **63**, 094406 (2001).

[16] K. A. Matveev, Phys. Rev. Lett. **92**, 106801 (2004).

[17] K. A. Matveev, Phys. Rev. B **70**, 245319 (2004).

[18] R. B. Griffiths, Phys. Rev. **133**, A768 (1964).

[19] F. D. M. Haldane, Phys. Rev. Lett. **45**, 1358 (1980).

[20] V. E. Korepin, N. M. Bogoliubov, and A. G. Izergin, *Quantum Inverse Scattering Method and Correlation Functions* (Cambridge University Press, Cambridge, 1993), Chap. II.

[21] M. Ogata and H. Shiba, Phys. Rev. B **41**, 2326 (1990).

[22] M. Ogata, T. Sugiyama, and H. Shiba, Phys. Rev. B **43**, 8401 (1991).

[23] A. Furusaki and K. A. Matveev, Phys. Rev. B **52**, 16676 (1995).

[24] K. Kamide, Y. Tsukada, and S. Kurihara, cond-mat/0411600.

[25] See also D. Schmeltzer, Phys. Rev. B **65**, 193303 (2002).

[26] The Hamiltonian matrix $\hat{\mathcal{H}}$ is positive definite and the velocities u_ν are real if $(u_\uparrow + \tilde{g}_{4\uparrow} + \tilde{g}_{2\uparrow})(u_\downarrow + \tilde{g}_{4\downarrow} + \tilde{g}_{2\downarrow}) > (\tilde{g}_{4\perp} + \tilde{g}_{2\perp})^2$ and $(u_\uparrow + \tilde{g}_{4\uparrow} - \tilde{g}_{2\uparrow})(u_\downarrow + \tilde{g}_{4\downarrow} - \tilde{g}_{2\downarrow}) > (\tilde{g}_{4\perp} - \tilde{g}_{2\perp})^2$. These are achieved if the parameters $\tilde{g}_{i\lambda,\perp}$ are not too large compared to the velocities u_λ. We note that the conditions are satisfied in the Hubbard model for arbitrary values of the coupling U/t, electron density n, and magnetization m.